remote sensing

MDPI

Article

Spatiotemporal Distribution Patterns and Exposure Risks of $PM_{2.5}$ Pollution in China

Jun Song [1,2], Chunlin Li [1,*], Miao Liu [1], Yuanman Hu [1] and Wen Wu [3]

[1] CAS Key Laboratory of Forest Ecology and Management, Institute of Applied Ecology, Chinese Academy of Sciences, Shenyang 110016, China; songjun990425@163.com (J.S.); lium@iae.ac.cn (M.L.); huym@iae.ac.cn (Y.H.)
[2] College of Geography and Environment, Shandong Normal University, Jinan 250300, China
[3] Jangho Architecture College, Northeastern University, Shenyang 110819, China; wuwen@mail.neu.edu.cn
* Correspondence: lichunlin@iae.ac.cn

Abstract: The serious pollution of $PM_{2.5}$ caused by rapid urbanization in recent years has become an urgent problem to be solved in China. Annual and daily satellite-derived $PM_{2.5}$ datasets from 2001 to 2020 were used to analyze the temporal and spatial patterns of $PM_{2.5}$ in China. The regional and population exposure risks of the nation and of urban agglomerations were evaluated by exceedance frequency and population weight. The results indicated that the $PM_{2.5}$ concentrations of urban agglomerations decreased sharply from 2014 to 2020. The region with $PM_{2.5}$ concentrations less than 35 $\mu g \cdot m^{-3}$ accounted for 80.27% in China, and the average $PM_{2.5}$ concentrations in 8 urban agglomerations were less than 35 $\mu g \cdot m^{-3}$ in 2020. The spatial distribution pattern of $PM_{2.5}$ concentrations in China revealed higher concentrations to the east of the Hu Line and lower concentrations to the west. The annual regional exposure risk (RER) in China was at a high level, with a national average of 0.75, while the average of 14 urban agglomerations was as high as 0.86. Among the 14 urban agglomerations, the average annual RER was the highest in the Shandong Peninsula (0.99) and lowest in the Northern Tianshan Mountains (0.76). The RER in China has obvious seasonality; the most serious was in winter, and the least serious was in summer. The population exposure risk (PER) east of the Hu Line was significantly higher than that west of the Hu Line. The average PER was the highest in Beijing-Tianjin-Hebei (4.09) and lowest in the Northern Tianshan Mountains (0.71). The analysis of air pollution patterns and exposure risks in China and urban agglomerations in this study could provide scientific guidance for cities seeking to alleviate air pollution and prevent residents' exposure risks.

Keywords: regional exposure risk; population exposure risk; $PM_{2.5}$; spatiotemporal pattern; urban agglomerations

Citation: Song, J.; Li, C.; Liu, M.; Hu, Y.; Wu, W. Spatiotemporal Distribution Patterns and Exposure Risks of $PM_{2.5}$ Pollution in China. *Remote Sens.* **2022**, *14*, 3173. https://doi.org/10.3390/rs14133173

Academic Editor: Riccardo Buccolieri

Received: 31 May 2022
Accepted: 30 June 2022
Published: 1 July 2022

1. Introduction

In the decades since the reform and opening up, China's rapid economic development, urbanization and population have caused severe damage to air quality [1]. Meanwhile, the major fossil energy consumption of transportation, industry, and residents' living needs is a direct source of $PM_{2.5}$ pollution, which has further exacerbated the problem of air pollution characterized by atmospheric particulate matter [2,3]. $PM_{2.5}$ refers to fine particulate matter with a dynamic diameter less than 2.5 μm, which is composed of a variety of complex chemical substances discharged from various natural and anthropogenic sources [4]. $PM_{2.5}$ is an important air pollutant that poses serious risks to public health all over the world and has become an issue of widespread concern to scientists and residents [5]. Since 2000, the Chinese government has issued a series of air pollution control policies, such as the 12th five-year plan on prevention and control of air pollution in key regions, the air pollution prevention and control action plan, and the three-year action plan for the defense of the blue sky [6–8]. Although many policies and measures have been taken and

air pollution has been significantly reduced, it has not yet reached the $PM_{2.5}$ pollution standard stipulated by the World Health Organization (WHO).

The temporal and spatial distribution patterns of $PM_{2.5}$ in China have been analyzed by many previous studies. Cheng et al., (2019) analyzed aerosol particle measurements in Southeast China from 2001 to 2016 and found that the $PM_{2.5}$ concentration showed a significant downward trend [9]. Using the spatiotemporal extra tree model, Wei et al., (2021) concluded that the air quality in the Pearl River Delta and the Yangtze River Delta improved significantly, and the pollution in the North China Plain was serious [10]. Jin et al., (2020) illustrated that the spatial pattern of $PM_{2.5}$ exposure maintained a stable structure over the Beijing-Tianjin-Hebei (BTH) region's distinct terrain, which has been described as "high in the northwest, low in the southeast" [11]. Wang et al., (2020) revealed that $PM_{2.5}$ presented a step-shaped decline from northwest to southeast in space and significant multiscale temporal variations in the Yangtze River Delta Urban Agglomeration during recent decades [12].

Urban agglomeration refers to the spatial layout pattern formed by different numbers and sizes of cities gathered within a certain spatial range, in which the population, production and economic activities are closely related [13]. The dense population, intense enterprise production and human activities in the urban agglomeration aggravate regional air pollution. Relevant studies revealed that there was a significant positive spatial correlation between $PM_{2.5}$ concentration and urbanization [14–16], and exploring the relationship between urban agglomerations and $PM_{2.5}$ has become a hot topic for urban sustainable development [17]. Many previous studies on $PM_{2.5}$ pollution from the perspective of urban agglomeration have mainly focused on the eastern coastal urban agglomerations of China. Wang and Fang (2016) studied the temporal and spatial distribution of $PM_{2.5}$ in the Bohai Rim urban agglomeration and indicated that the $PM_{2.5}$ concentration was high in southern Hebei and western Shandong in winter and autumn, and the per capita GDP, urbanization rate and urban construction had greater impacts on $PM_{2.5}$ [18]. Wu et al., (2021) evaluated the spatial distribution of nine Chinese key urban agglomerations by using spatial autocorrelation analysis and dynamic time warping and reported that from 2000 to 2017, the $PM_{2.5}$ concentration first increased and then fluctuated and decreased, and the concentration was high in the plains areas where the core cities of urban agglomerations were located [19].

According to epidemiological studies, air pollution, especially $PM_{2.5}$, has different kinds and degrees of impact on the human body [20]. $PM_{2.5}$ pollution ranks sixth among all risk factors for global early death rate and disability-adjusted life years [21], posing serious threats to the life and health of residents. Exposure to $PM_{2.5}$ directly increases the risks of stroke, ischemic heart disease, chronic obstructive pulmonary disease, and lung cancer and can lead to premature death [4,21,22]. It can also lead to metabolic disorders and aggravate other chronic diseases [23]. Liu et al., (2016) predicted that the number of diseases directly caused by exposure to $PM_{2.5}$ in China was 1.37 million, including stroke (690,000), ischemic heart disease (380,000), lung cancer (130,000) and chronic obstructive pulmonary disease (170,000) [24]. Air pollution is closely related to different aspects of mental health, and the acceptable public risk rate decreases as the $PM_{2.5}$ concentration increases [25]. Wang et al., (2021) reported that the $PM_{2.5}$ concentration in urban areas decreased by 42.95% between 2013 and 2018, and the premature deaths in long- and short-term $PM_{2.5}$ exposure decreased by 10.13% and 72.49%, respectively, in 2018 compared with 2013 [26]. Song et al., (2019) indicated that approximately half of the population living in the BTH region was exposed to monthly mean $PM_{2.5}$ concentrations greater than $80 \mu g \cdot m^{-3}$ in 2015, and the premature deaths of all causes and from cardiovascular and respiratory diseases attributed to $PM_{2.5}$ were estimated to be 138,150, 80,945, and 18,752, respectively [27]. Fu et al., (2020) used the exposure response relationship model to analyze the impact of $PM_{2.5}$ on health from 2015 to 2017 and found that the health effect economic loss (mainly caused by chronic bronchitis and premature death) accounted for 1.73%, 1.53% and 1.41% of GDP in these years, respectively [28]. The carcinogenic risk caused by exposure to $PM_{2.5}$ has obvious

urban–rural differences. With increased $PM_{2.5}$ exposure, the risks for ovarian and prostate cancer rise significantly in urban areas, while risks for lung cancer and leukemia rise significantly in rural areas [29].

Over the past two decades, China's economy and society have developed rapidly, and intense industrialization and urbanization have led to serious air pollution, especially the $PM_{2.5}$ pollution in urban agglomerations. As urban agglomerations have a concentrated population distribution, a large number of people in these areas are exposed to high concentrations of $PM_{2.5}$. In this study, ground-level $PM_{2.5}$ data of China with a spatial resolution of 1 km from 2001 to 2020 were used to investigate the spatiotemporal distribution patterns and exposure risks. The main purposes of this study were (1) to reveal the temporal and spatial distribution of $PM_{2.5}$ concentrations in China from 2001 to 2020 and (2) to analyze the regional and population exposure risks of China and 14 urban agglomerations. The methods and results in this study are expected to deepen the understanding of $PM_{2.5}$ exposure risks under changes in pollution patterns and population distributions in China and provide a theoretical basis for policies to improve air quality and alleviate residents' air pollution exposure risks.

2. Materials and Methods

2.1. Study Area

The study area of this research is China and its 14 major urban agglomerations. Among the selected urban agglomerations, 13 are distributed east of the Hu Line, and 1 is distributed west of the Hu Line (Figure 1). The Hu Line, also known as the "Hu Huanyong Line", is an imaginary line stretching from Heihe (a city in northern China located on the Russian border) to Tengchong (a southwestern city bordering Myanmar), which divides the area of China into two roughly equal parts [30]. The Hu Line is also recognized as the dividing line of China's ecological environment, socioeconomic development, population distribution and urbanization level [31–33].

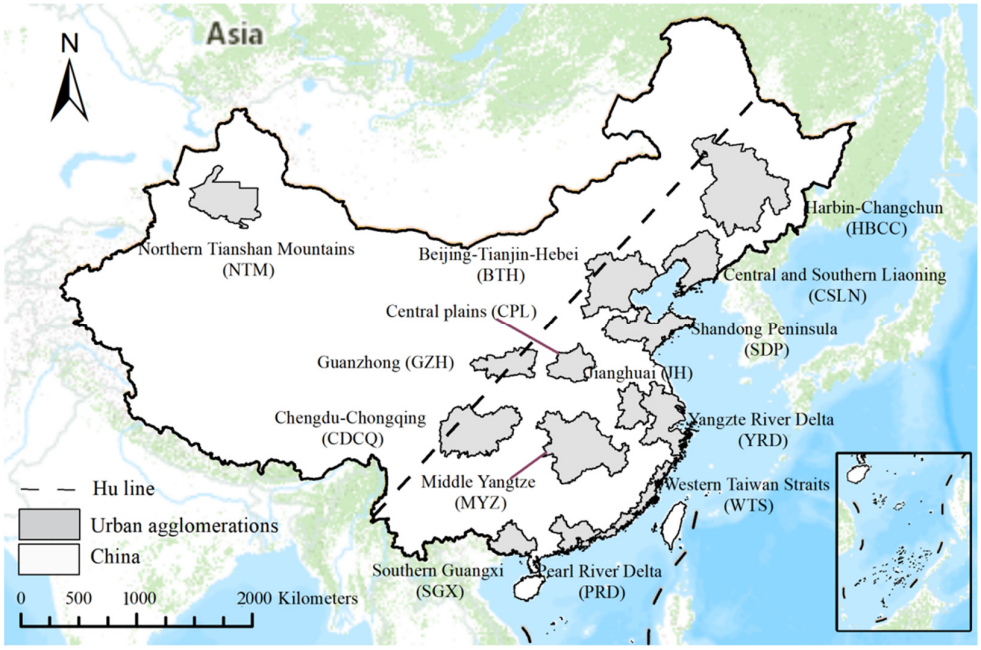

Figure 1. China and 14 urban agglomerations. Abbreviations for the 14 urban agglomerations: Beijing-Tianjin-Hebei (BTH), Central and Southern Liaoning (CSLN), Harbin-Changchun (HBCC), Shandong Peninsula (SDP), Jianghuai (JH), Yangtze River Delta (YRD), Western Taiwan Straits (WTS), Middle Yangtze (MYZ), Pearl River Delta (PRD), Southern Guangxi (SGX), Chengdu-Chongqing (CDCQ), Guanzhong (GZH), Central Plains (CPL) and Northern Tianshan Mountains (NTM).

Among the 14 major urban agglomerations, there are five national urban agglomerations, including the Yangtze River Delta (YRD), Pearl River Delta (PRD), Beijing-Tianjin-Hebei (BTH), Middle Yangtze (MYZ), and Chengdu-Chongqing (CDCQ), accounting for 9.06%, 31.39% and 46.48% of the total land area, population and GDP in China, respectively. The others are regional urban agglomerations, including Harbin-Changchun (HBCC), Central and Southern Liaoning (CSLN), Shandong Peninsula (SDP), Western Taiwan Straits (WTS), Central Plains (CPL), Guanzhong (GZH), Southern Guangxi (SGX), Jianghuang (JH), and Northern Tianshan Mountains (NTM), accounting for 9.84%, 24.67% and 28.00% of the total land area, population and GDP in China, respectively [34].

2.2. Data

2.2.1. Ground-Level $PM_{2.5}$ Data

The PM data of China from 2001 to 2020 were obtained from the ChinaHigh$PM_{2.5}$ data set, with a spatial resolution of 1 km [10,35]. ChinaHigh$PM_{2.5}$ is one of a series of long-term, full-coverage, high-resolution, and high-quality datasets of ground-level air pollutants for China. Considering the spatiotemporal heterogeneity of air pollution, the $PM_{2.5}$ concentration at 1 km resolution was estimated by using the spatiotemporal extra tree (STET) model and the atmospheric correction (MAIAC) algorithm. At the same time, auxiliary data that may affect $PM_{2.5}$ concentration, including meteorological variables, surface conditions, pollutant emissions and population distribution, were collected to improve data accuracy. In the evaluation process, several main meteorological variables were analyzed and extracted from ERA-Interim, including temperature, relative humidity, precipitation, evaporation, surface pressure, wind speed and wind direction. The results showed that the dataset captured variations in $PM_{2.5}$ concentrations at different spatiotemporal scales well, with higher accuracies (cross-validation coefficient of determination, CV-R^2 = 0.86–0.90) and stronger predictive powers (R^2 = 0.80–0.82) than previously reported. The annual average $PM_{2.5}$ concentration data were used to analyze the changes in the pollutant interannual distribution pattern and exposure risk, and the daily average $PM_{2.5}$ concentration data of 2020 were used to analyze the changes in the pollutant seasonal distribution pattern and exposure risk.

2.2.2. Population Density Data

The population density from 2001 to 2020 in China was obtained from the Worldpop gridded population dataset (https://www.worldpop.org/methods/populations (accessed on 1 March 2022). The resolution of this dataset is 30 arc seconds, which is about 1 km for longitude resolution and latitude resolution at the equator. The population density data were used to calculate the population exposure risks under the condition of different population distributions.

2.3. Method

2.3.1. Trend Analysis

Ordinary least-squares regression is widely used in trend analysis of sequence data evolution. In this study, trend analysis was used to characterize the change trends of annual $PM_{2.5}$ concentrations from 2001 to 2020 and determine the degree of its increase or decrease. The calculation formula is:

$$T = \frac{n\sum_{i=1}^{n}(i \times p_i) - (\sum_{i=1}^{n} i) \times (\sum_{i=1}^{n} p_i)}{n\sum_{i=1}^{n} i^2 - (\sum_{i=1}^{n} i)^2} \quad (1)$$

where T is the change trends of the $PM_{2.5}$ concentration of each grid, n is the time span, i is the number of years, and pi is the annual average concentration of $PM_{2.5}$ in the ith year. If

T is greater than 0, it indicates that the $PM_{2.5}$ concentration has an increasing trend; if T is less than 0, it indicates that the $PM_{2.5}$ concentration has a decreasing trend.

$$r = \frac{\sum_{i=1}^{n}(p_i - \overline{p}) \times (t_i - \overline{t})}{\sqrt{\sum_{i=1}^{n}(p_i - \overline{p})^2} \times \sqrt{\sum_{i=1}^{n}(t_i - \overline{t})^2}} \quad (2)$$

where r is the correlation coefficient; t is the time series from 1 to 20; and $\overline{p}$ and $\overline{t}$ are the mean values of p and t, respectively. The value of r ranges from -1 to 1.

2.3.2. Regional Exposure Risk Analysis

The regional exposure risk (RER) of air pollution refers to the time when the air pollutant concentration exceeds the limitation in a region, which reflects the length or proportion of time people in this region are exposed to air pollution. The exceedance frequency was used to estimate the annual and seasonal RER of $PM_{2.5}$, and the calculation formula is:

$$RER_j = \frac{count(C_j > S)}{n} \quad (3)$$

where RER_j is the *RER* of $PM_{2.5}$ in grid j; C_j is the $PM_{2.5}$ concentration in grid j; S is the interim target 1 (IT-1) of the WHO; the IT-1 for annual $PM_{2.5}$ concentration is 35 $\mu g \cdot m^{-3}$, and that for daily $PM_{2.5}$ concentration is 75 $\mu g \cdot m^{-3}$. The annual and seasonal *RERs* were calculated based on the annual $PM_{2.5}$ concentration and daily $PM_{2.5}$ concentration, respectively. n represents the time span, which is years for annual *RER* and days of each season for seasonal *RER*. The value of *RER* ranges from 0 to 1. A value of 0 indicates that there is no event exceeding the pollution standard of IT-1, while the larger the value of *RER* is, the greater the proportion of pollution events, and a value of 1 means that the $PM_{2.5}$ concentration exceeds the standard of IT-1 throughout the whole period.

2.3.3. Population Exposure Risk Analysis

High concentrations of $PM_{2.5}$ pose serious threats to human life and health. However, due to the uneven distribution of population density, the RER cannot fully reflect the exposure risk of $PM_{2.5}$ for residents. To solve this problem, it is necessary to quantify the risk under different population densities. In this study, population exposure risk (PER) was used to quantify the population exposure risk of $PM_{2.5}$ pollution on a spatial scale. The calculation formula is:

$$PER_{ij} = \frac{P_{ij} \times C_{ij}}{\left(\sum_{j=1}^{m}(P_{ij} \times C_{ij})\right)/m} \quad (4)$$

where PER_{ij} is the *PER* of $PM_{2.5}$ in grid j in the ith year, C_{ij} is the average annual $PM_{2.5}$ concentration of grid j in the ith year, P_{ij} is the population density of grid j in the ith year, and m is the total number of grids in the study area. *PER* was divided into five levels, including level 0 ($0 \leq PER \leq 1$), level 1 ($1 < PER \leq 2$), level 2 ($2 < PER \leq 3$), level 3 ($3 < PER \leq 5$) and level 4 ($PER > 5$).

3. Results

3.1. Distribution Patterns of $PM_{2.5}$ Concentrations

The temporal and spatial distribution patterns of annual average $PM_{2.5}$ from 2001 to 2020 were calculated by annual ground-level $PM_{2.5}$ data. The distribution patterns of $PM_{2.5}$ concentrations in 5 representative years are displayed in Figure 2. Over the past 20 years, the distribution patterns of $PM_{2.5}$ in China have been roughly divided by the Hu Line. The $PM_{2.5}$ concentration in the eastern region was higher, and the concentration in the western region was lower, except for the Tarim Basin in Western China. From the overall distribution of $PM_{2.5}$ concentrations in the five representative years, it can be clearly found that the $PM_{2.5}$ pollution in most regions of China was obviously reduced from 2001 to 2020.

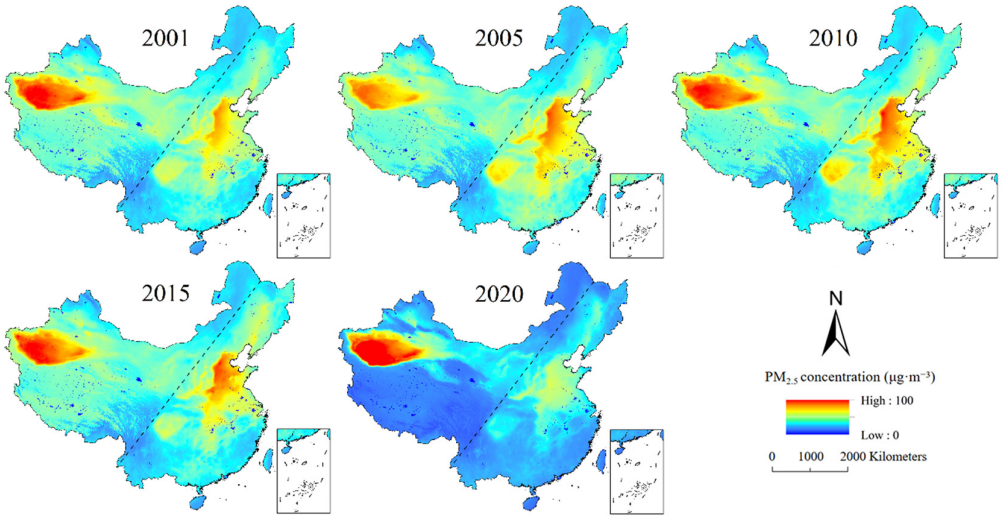

Figure 2. Temporal and spatial distribution patterns of annual average $PM_{2.5}$ concentrations in 5 representative years in China.

Based on the WHO global air quality guidelines, the IT-1 of the annual average $PM_{2.5}$ (35 $\mu g \cdot m^{-3}$) was used as the standard. The value range of $PM_{2.5}$ was divided into four categories according to the IT-1 value, which were <35 $\mu g \cdot m^{-3}$, 35–70 $\mu g \cdot m^{-3}$, 70–105 $\mu g \cdot m^{-3}$, and >105 $\mu g \cdot m^{-3}$. The area proportion of each category in the past 20 years is shown in Figure 3a. From 2001 to 2014, the area with $PM_{2.5}$ concentrations less than 35 $\mu g \cdot m^{-3}$ accounted for a small proportion (approximately 6.49%), while the concentrations in most areas were between 35 and 70 $\mu g \cdot m^{-3}$ (79.57%). Since 2015, the proportion of regions with $PM_{2.5}$ concentrations of less than 35 $\mu g \cdot m^{-3}$ has increased considerably, from 7.06% in 2014 to 80.27% in 2020. The area with $PM_{2.5}$ concentrations between 35 and 70 $\mu g \cdot m^{-3}$ decreased accordingly, from 82.69% in 2014 to 14.98% in 2020. The area with $PM_{2.5}$ concentrations greater than 75 $\mu g \cdot m^{-3}$ decreased slightly, from 7.46% in 2001 to 4.38% in 2020. The changes in the $PM_{2.5}$ concentrations of 14 urban agglomerations over the past 20 years revealed that the $PM_{2.5}$ concentrations of urban agglomerations decreased sharply from 2014 to 2020 (Figure 3b). In particular, the concentrations in most urban agglomerations, except GZH, JH, BTH, CSLN, SDP and CPL, decreased below the specified limit of 35 $\mu g \cdot m^{-3}$ in 2020.

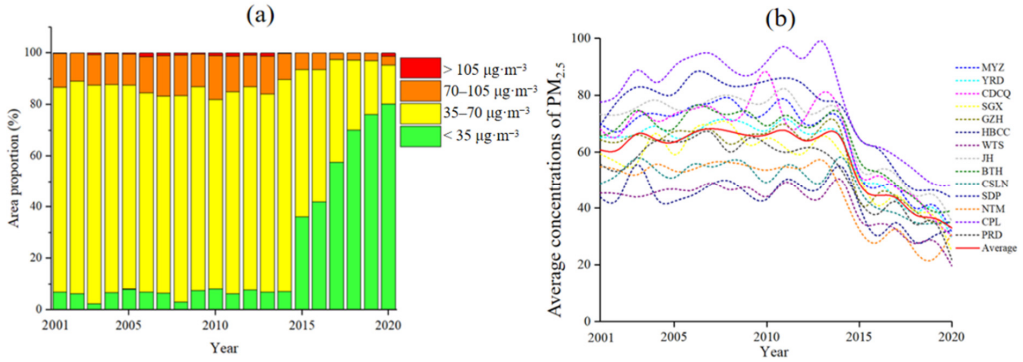

Figure 3. Temporal and spatial patterns of $PM_{2.5}$ concentrations from 2001 to 2020. (**a**) Area proportion of 4 categories of $PM_{2.5}$ concentrations in China; (**b**) average concentrations of $PM_{2.5}$ in 14 urban agglomerations.

From 2001 to 2020, the concentrations of $PM_{2.5}$ in 14 urban agglomerations showed two obvious categories, with different trends (Table 1). In the first stage (2001–2014), the concentration did not decrease significantly, and even seemed to increase with the passage of time for some urban agglomerations. Both the increase and decrease were small. In the second stage (2015–2020), 14 urban agglomerations showed an obvious downward

trend. Among them, CDCQ (−6.14 μg·m^{-3}/year), MYZ (−5.65 μg·m^{-3}/year) and JH (−5.47 μg·m^{-3}/year) decreased the most, while NTM (−2.24 μg·m^{-3}/year) and HBCC (−3.30 μg·m^{-3}/year) decreased the least. It can be seen that the relevant policies adopted by China to control $PM_{2.5}$ in recent years have achieved remarkable results.

Table 1. Characteristics of two stages of $PM_{2.5}$ concentrations in 14 urban agglomerations from 2001 to 2020.

Regions	$PM_{2.5}$ in 2001 (μg·m^{-3})	$PM_{2.5}$ in 2014 (μg·m^{-3})	$PM_{2.5}$ in 2020 (μg·m^{-3})	Average Change from 2001 to 2014 (μg·m^{-3})	Average Change from 2015 to 2020 (μg·m^{-3})
MYZ	70.14	71.08	31.54	0.07	−5.65
PRD	65.20	65.62	29.37	0.03	−5.18
CDCQ	68.12	73.34	30.36	0.37	−6.14
SGX	59.40	59.95	24.71	0.04	−5.03
GZH	64.36	67.48	35.07	0.22	−4.63
HBCC	43.87	55.12	32.05	0.80	−3.30
WTS	45.33	50.31	19.71	0.36	−4.37
JH	73.25	73.60	35.30	0.02	−5.47
BTH	65.60	73.37	39.07	0.56	−4.90
CSLN	48.82	58.29	35.20	0.68	−3.30
SDP	69.48	76.47	43.67	0.50	−4.69
NTM	54.89	46.77	31.11	−0.58	−2.24
CPL	77.62	81.15	48.26	0.25	−4.70
PRD	55.76	54.08	21.90	−0.12	−4.60
Average	60.83	65.08	32.99	0.30	−4.58

3.2. Distribution Patterns of $PM_{2.5}$ Trends

The change trends of annual $PM_{2.5}$ concentrations from 2001 to 2020 were explored by the ordinary least-squares regression method, and the spatial distribution of trends is presented in Figure 4. The T value was negative in most regions of China, indicating that the $PM_{2.5}$ concentration has gradually decreased in the past two decades (Figure 4a). The area with a significant decrease ($p < 0.05$) in the $PM_{2.5}$ concentration accounted for 86.34% of the total national area (Figure 4b). There were few areas with significant ($p < 0.05$) and nonsignificant ($p \geq 0.05$) increases in $PM_{2.5}$ concentrations, accounting for 0.05% and 3.13% of the national area, respectively, and they were mainly concentrated in Western China. For urban agglomerations, except NTM, the $PM_{2.5}$ concentration in other urban agglomerations illustrated a complete decreasing trend (Figure 4c). The trends of $PM_{2.5}$ concentration in SGX, PRD and WTS showed a significant decrease, and other urban agglomerations revealed a significant and nonsignificant decrease from 2001 to 2020.

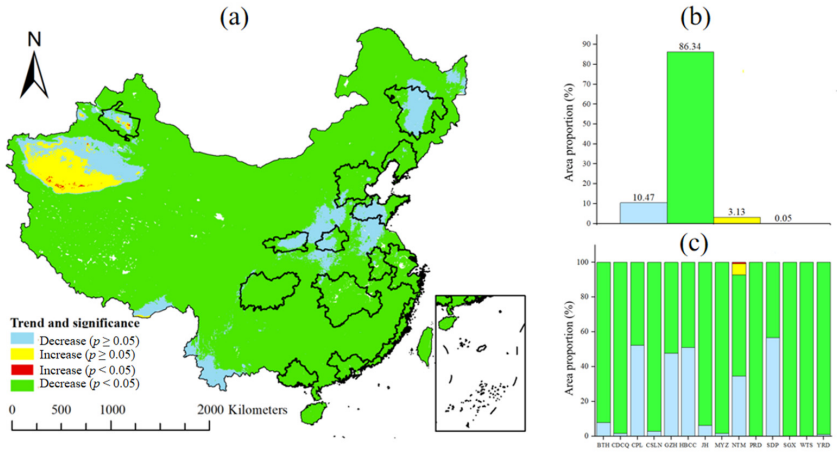

Figure 4. Spatial distribution patterns of the $PM_{2.5}$ trend in China and 14 urban agglomerations. (**a**) Distribution of trend and significance in China and 14 urban agglomerations; (**b**) area proportion of 4 categories of $PM_{2.5}$ trend in China; (**c**) area proportion of 4 categories of $PM_{2.5}$ trend in 14 urban agglomerations.

3.3. Regional Exposure Risks of $PM_{2.5}$

The annual RERs of the $PM_{2.5}$ concentration in China and 14 urban agglomerations from 2001 to 2020 are presented in Figure 5. Overall, the annual RER in China was at a high level, with a national average of 0.75, while the average of 14 urban agglomerations was as high as 0.86. The annual RERs in Central, Eastern and Northwest China were the highest, and those in Northeast and Southwest China were the lowest (Figure 5a). Among the 14 urban agglomerations, the average annual RER was the highest in SDP (0.99), followed by CPL (0.98) and JH (0.97), and the lowest annual RERs were in WTS (0.79), HBCC (0.78) and NTM (0.76) (Figure 5b).

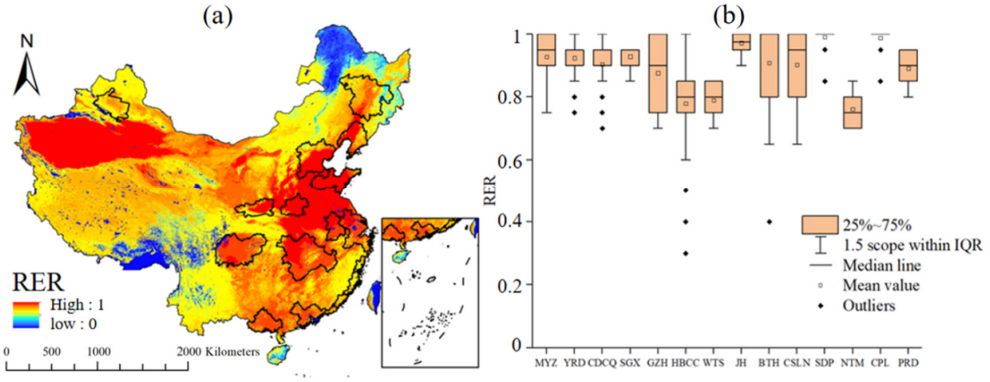

Figure 5. Regional exposure risks of $PM_{2.5}$ concentrations in China and 14 urban agglomerations. (**a**) Distribution of regional exposure risks in China and 14 urban agglomerations; (**b**) regional exposure risks of 14 urban agglomerations.

To analyze the RER of $PM_{2.5}$ concentrations in each season, the 24 h average concentration limitation (75 $\mu g \cdot m^{-3}$) of WHO's IT-1 was set as the standard. The proportion of days exceeding the limitation in each season of 2020 was calculated, and the results of the seasonal RER are presented in Figure 6. The RER in China has obvious seasonality; the most serious was winter, and the least serious was summer. Among the different urban agglomerations, the RER of HBCC in spring was the highest (0.08). In summer, except for MYZ, for which the RER was 0.05, the RERs of the other urban agglomerations were very low. The high RER values in autumn were mainly concentrated in Central and Eastern China, where the RERs of BTH, SDP and CPL were relatively high. In winter, the RERs of all urban agglomerations except SGX and WTS were high, and the highest RER was in CPL (0.49). The RERs of SGX, WTS and PRD along the southern coast of China were low throughout the year. The RERs of HBCC, NTM and CSLN in northern China were higher in spring and winter.

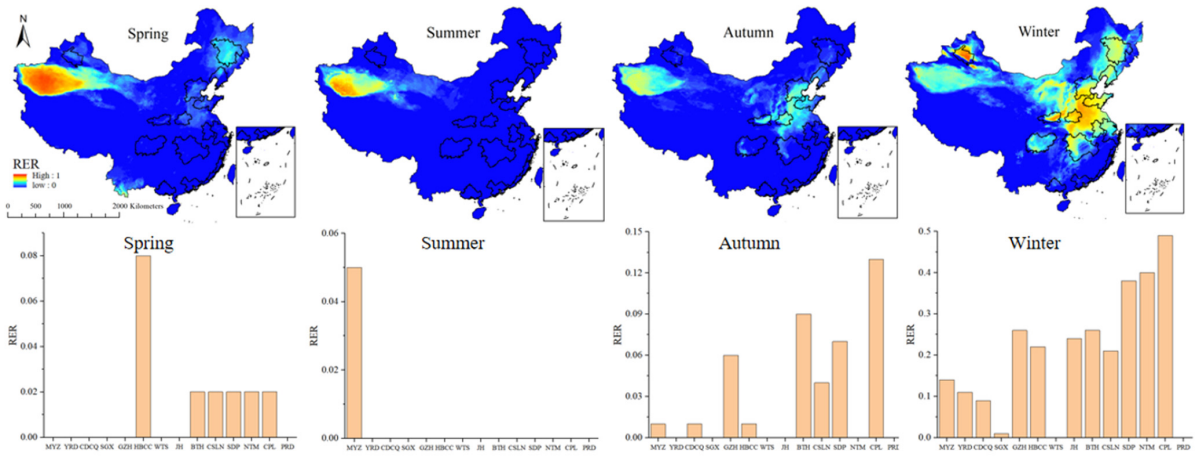

Figure 6. Regional exposure risk of $PM_{2.5}$ concentrations in each season in 2020.

3.4. Population Exposure Risks of $PM_{2.5}$

The PERs of $PM_{2.5}$ concentrations in China and 14 urban agglomerations from 2001 to 2020 are presented in Figure 7. The PERs of the 14 urban agglomerations showed a fluctuating trend, with no significant change in 20 years. The average PER of urban agglomerations was higher than that of China as a whole. Among the 14 urban agglomerations, the PERs of BTH, YRD, SDP and CPL were higher, while the PERs of CSLN, HBCC and NTM were lower than the national average.

Figure 7. Population exposure risks of $PM_{2.5}$ in China and 14 urban agglomerations from 2001 to 2020.

Since the PER from 2001 to 2020 was basically the same, the PER distribution pattern of China and urban agglomerations was analyzed by using the PER in 2020 (Figure 8). The PER east of the Hu Line was significantly higher than that west of the Hu Line, and the PER in the eastern coastal and central regions was higher (Figure 8a). Among the 14 urban agglomerations, the average PER was the highest in BTH (4.09), followed by YRD (3.75), SDP (2.91) and CPL (2.9), and the lowest in CSLN (0.85), HBCC (0.76) and NTM (0.71) (Figure 8b). The PER level east of the Hu Line was higher than that west of the Hu Line (Figure 8c). The PERs of urban agglomerations were higher than those of other regions. For 14 urban agglomerations, BTH, YRD, SDP and CPL have the highest risk level of PER, and level 3 and level 4 account for the largest proportion. SGX, CSLN, HBCC and NTM have the lowest risk level of PER, with the largest proportions at level 0, level 1 and level 2 (Figure 8d).

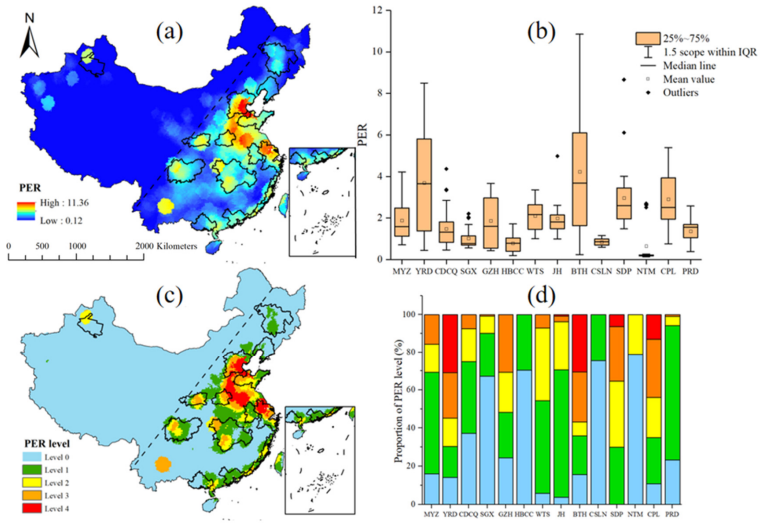

Figure 8. Distribution and classification of population exposure risks of $PM_{2.5}$ in 2020. (**a**) Population exposure risks in China and 14 urban agglomerations in 2020; (**b**) population exposure risks of 14 urban agglomerations; (**c**) population exposure risk classification in China and 14 urban agglomerations in 2020; (**d**) area proportion of population exposure risk in five levels of urban agglomerations.

4. Discussion

4.1. Influencing Factors of the Evolution of $PM_{2.5}$ Distribution

The distribution patterns of $PM_{2.5}$ concentrations in China illustrated obvious regional differences. The general trend of $PM_{2.5}$ distributions in China is high in the East and low in the West. $PM_{2.5}$ concentration is closely related to urbanization level, energy use, production mode, population density, etc. [36–38]. From 2001 to 2010, $PM_{2.5}$ in China rose rapidly, especially in eastern China [39]. Due to large population, energy consumption, frequent economic activities and rapid urbanization process, the $PM_{2.5}$ concentration in eastern China maintained at a high level. Subsequently, the Chinese government realized the serious harm caused by $PM_{2.5}$ and began to adopt a series of policies to reduce $PM_{2.5}$ concentration to balance the relationship between economic development and pollution emissions [7].Therefore, $PM_{2.5}$ concentrations in China began to decrease significantly, especially after 2013.Due to the dust transported by the Taklimakan Desert and the Kunlun Mountains block the northeast wind, the $PM_{2.5}$ concentration in Taklimakan Desert in Xinjiang (yellow area in the Figure 4a) is unstable from 2001 to 2020 [40,41], therefore, the results showed an upward trend ($p > 0.05$).

Meanwhile, there were seasonal differences of $PM_{2.5}$ concentrations in China. The $PM_{2.5}$ concentrations in densely populated areas of North China were significantly higher than those in other areas. Due to the cold winter weather in northern China, coal-fired heating is an important pollution emission source, emitting a large amount of fine particulates, sulfides and nitrogen oxides [42]. In addition, straw burning in agricultural planting areas is also an important factor in seasonal $PM_{2.5}$ pollution [43].

The outbreak of COVID-19 pandemic in 2020 has brought abnormal impact on the analysis of air quality. In different cities and regions in China, $PM_{2.5}$ is significantly affected by COVID-19 [44]. In response to the epidemic, China has adopted the city closure policy, reducing human activities and some economic production, resulting in a decrease of $PM_{2.5}$ concentration in some areas. Wuhan, the most severely affected city, was blocked for 76 days, and the $PM_{2.5}$ concentration decreased by 35% compared with the same period in previous years [45]. However, the closure of the city does not strictly mean the reduction of pollution, which may cause a significant impact on the short-term air pollution [46]. For example, during the COVID-19 blockade, severe haze still occurred in northern China due to high relative humidity and poor air [47]. Other factors such as transportation and secondary pollution offset the reduction of $PM_{2.5}$ concentration [48].

Meteorology is an important factor affecting $PM_{2.5}$ pollution. $PM_{2.5}$ is negatively correlated with daily temperature, relative humidity, precipitation and wind speed, and positively correlated with atmospheric pressure [49]. However, atmospheric circulation is conducive to the dissipation of $PM_{2.5}$ [50]. At the same time, $PM_{2.5}$ concentration is affected by traffic. The most important local factor causing air pollution is the exhaust gas emitted by road vehicles, especially heavy diesel powered vehicles [51]. In addition, tire wear, road dust resuspension, traffic facilities area, road width and length also affect $PM_{2.5}$ concentration [52–54].

4.2. Exposure Risk Characteristics and Evaluation Methods

Two methods based on exceedance frequency and population weight were used to evaluate the exposure risk in China. For RER, all of China was at a high-risk level, with an annual average of 0.75, while the average of 14 urban agglomerations was as high as 0.86. The RER in China has obvious seasonality; the most serious occurs in winter and the least serious in summer. The PERs of $PM_{2.5}$ east of the Hu Line were obviously higher than those west of the Hu Line. The PER of urban agglomeration was higher, and that of other regions was at a lower level. The great differences in PER distribution patterns are mainly due to the dense population in the east and sparse population in the west in China [55].

RER and PER have both advantages and disadvantages in assessing the exposure risks of air pollution. RER provides a better understanding and a better basis for the spatial management of pollution prevention. Due to the vulnerability of air pollutants

to climate, $PM_{2.5}$ in a certain area may vary greatly in different years [56]. This study uses 20 years of data to calculate the multiyear cumulative RER to provide a long-term mechanism for formulating management strategies to improve air quality as additional information beyond the widely accepted global disease burden research [57]. However, RER ignores the uneven spatial distribution of the population, which makes it difficult to reflect the difference in exposure risk in areas with different population densities under the same $PM_{2.5}$ concentration [58]. And many previous studies revealed that the severity of $PM_{2.5}$ pollution is closely related to population density [59]. PER considers the spatial distribution of the population and compares the exposure risks in different regions [60]. To assess the level of $PM_{2.5}$ exposure risk, especially in specific regions, it is more appropriate to use PER which considering the population distribution [61]. Therefore, due to the uneven distribution of China's population, PER seems to be a more appropriate method for assessing $PM_{2.5}$ exposure risks in China.

4.3. Advantages and Limitations

Due to the development of remote sensing technology, high time resolution remote sensing products promote the application of environmental issue analysis. In this study, daily average $PM_{2.5}$ concentration data were used to assess the seasonal variation in exposure risks. Moreover, the RER and PER were proposed to comprehensively evaluate the exposure risk of air pollution, and this assessment and analysis framework can avoid the deviation of risk estimation by a single index. Urban agglomerations are the areas with the most intense human activities, so the analysis of air pollution patterns and exposure risks of urban agglomerations in this study could provide scientific guidance to help cities alleviate air pollution and prevent residents' exposure risks. The air pollution data obtained from fixed meteorological stations and mobile monitoring can better reflect the pollution distribution pattern and exposure risk [62,63]. However, due to the limited number of monitoring stations, the monitoring data based on stations cannot meet the spatial resolution requirements [64,65]. Due to the wide space and time coverage of satellite observations, remote sensing estimation of $PM_{2.5}$ concentration is a powerful supplement to the limited ground observations [66], but may be different from the real pollutant concentration near the ground. Therefore, a model considering both monitoring station and satellite remote sensing data was a good choice [27]. The ChinaHigh$PM_{2.5}$ dataset used in this paper used the STET model, which contained auxiliary information about meteorological variables, land use, pollutant emissions and population [10,35]. Therefore, compared with previous studies, the data used in this paper were more accurate and the research results were much more reliable.

In addition to the advantages of the methods and results of air pollution exposure risk assessment described above, there are some shortcomings. Population mobility, such as the population distribution during the day and at night, annual population migration, and Spring Festival transportation, will bring considerable uncertainty about the exposure risks of air pollution [67]. However, it is very difficult to obtain real-time dynamic population data, and with the development of science and technology, big data could help in this regard, such as mobile phone signaling data and software location data [68,69].

In this study, only the influence of $PM_{2.5}$ pollutant was considered, but there are other air pollutants that will cause adverse effects. China has a high incidence rate of asthma due to NO_2 exposure [70]. SO_2 will lead to the formation of haze, and increase the mortality and incidence rate of cardiopulmonary diseases [71]. In addition, there are atmospheric pollutants such as CO, CO_2 and PM_{10}, which also have a great impact on the environment and human health.

5. Conclusions

In this study, the $PM_{2.5}$ remote sensing inversion data and population density data of China from 2001 to 2020 were used to explore the $PM_{2.5}$ concentration distribution patterns and exposure risks. Regional and population exposure risks of $PM_{2.5}$ based on exceedance

frequency and population weight were proposed to evaluate the exposure risks in China and 14 urban agglomerations. The results indicated that the $PM_{2.5}$ concentrations of urban agglomerations decreased sharply from 2014 to 2020. The region with $PM_{2.5}$ concentrations less than 35 $\mu g \cdot m^{-3}$ accounted for 80.27% of the area of China, and the average $PM_{2.5}$ concentrations in 8 urban agglomerations were less than 35 $\mu g \cdot m^{-3}$ in 2020. The spatial distribution patterns of $PM_{2.5}$ concentrations in China were higher to the east of the Hu Line and lower to the west. The annual RER in China was at a high level, with a national average of 0.75, while the average of 14 urban agglomerations was as high as 0.86. Among the 14 urban agglomerations, the average annual RER was the highest in SDP (0.99), followed by CPL (0.98) and JH (0.97), and the lowest annual RERs were in WTS (0.79), HBCC (0.78) and NTM (0.76). The RER in China has obvious seasonality; the most serious was in winter, and the least serious was in summer. The PER east of the Hu Line was significantly higher than that west of the Hu Line, and the PER in the eastern coastal and central regions was higher. The average PER was the highest in BTH (4.09), followed by YRD (3.75), SDP (2.91) and CPL (2.9), and the lowest in CSLN (0.85), HBCC (0.76) and NTM (0.71). The analysis of air pollution patterns and exposure risks in China and urban agglomerations in this study could better provide scientific guidance to help cities alleviate air pollution, and reduce residents' exposure risks.

Author Contributions: Conceptualization, J.S. and C.L.; methodology, J.S. and M.L.; software, Y.H.; writing—original draft preparation, J.S.; writing—review and editing, C.L. and W.W. All authors have read and agreed to the published version of the manuscript.

Funding: This research was funded by the National Natural Science Foundation of China, grant number (Nos. 41871192, 41730647 and 32071580) and the Youth Innovation Promotion Association of CAS, grant number (2021194).

Institutional Review Board Statement: Not applicable.

Informed Consent Statement: Not applicable.

Data Availability Statement: The data presented in this study are available on request from the corresponding author.

Conflicts of Interest: The authors declare no conflict of interest.

References

1. Dong, F.; Li, J.; Li, K.; Sun, Z.; Yu, B.; Wang, Y.; Zhang, S. Causal chain of haze decoupling efforts and its action mechanism: Evidence from 30 provinces in China. *J. Clean. Prod.* **2020**, *245*, 118889. [CrossRef]
2. Guan, X.; Wei, H.; Lu, S.; Dai, Q.; Su, H. Assessment on the urbanization strategy in China: Achievements, challenges and reflections. *Habitat Int.* **2018**, *71*, 97–109. [CrossRef]
3. Wang, K.; Zhao, X.; Peng, B.; Zeng, Y. Can energy efficiency progress reduce $PM_{2.5}$ concentration in China's cities? Evidence from 105 key environmental protection cities in China, 2004–2015. *J. Clean. Prod.* **2021**, *288*, 125684. [CrossRef]
4. Yan, D.; Lei, Y.; Shi, Y.; Zhu, Q.; Li, L.; Zhang, Z. Evolution of the spatiotemporal pattern of $PM_{2.5}$ concentrations in China—A case study from the Beijing-Tianjin-Hebei region. *Atmos. Environ.* **2018**, *183*, 225–233. [CrossRef]
5. Tan, S.H.; Roth, M.; Velasco, E. Particle exposure and inhaled dose during commuting in Singapore. *Atmos. Environ.* **2017**, *170*, 245–258. [CrossRef]
6. Feng, L.; Liao, W. Legislation, plans, and policies for prevention and control of air pollution in China: Achievements, challenges, and improvements. *J. Clean. Prod.* **2016**, *112*, 1549–1558. [CrossRef]
7. Gao, J.; Yuan, Z.; Liu, X.; Xia, X.; Huang, X.; Dong, Z. Improving air pollution control policy in China—A perspective based on cost–benefit analysis. *Sci. Total. Environ.* **2016**, *543*, 307–314. [CrossRef]
8. Jiang, X.; Li, G.; Fu, W. Government environmental governance, structural adjustment and air quality: A quasi-natural experiment based on the Three-year Action Plan to Win the Blue Sky Defense War. *J. Environ. Manag.* **2021**, *277*, 111470. [CrossRef] [PubMed]
9. Cheng, B.; Wang-Li, L.; Meskhidze, N.; Classen, J.; Bloomfield, P. Spatial and temporal variations of $PM_{2.5}$ mass closure and inorganic $PM_{2.5}$ in the Southeastern U.S. *Environ. Sci. Pollut. Res.* **2019**, *26*, 33181–33191. [CrossRef] [PubMed]
10. Wei, J.; Li, Z.; Lyapustin, A.; Sun, L.; Peng, Y.; Xue, W.; Su, T.; Cribb, M. Reconstructing 1-km-resolution high-quality $PM_{2.5}$ data records from 2000 to 2018 in China: Spatiotemporal variations and policy implications. *Remote. Sens. Environ.* **2021**, *252*, 112136. [CrossRef]
11. Jin, N.; Li, J.; Jin, M.; Zhang, X. Spatiotemporal variation and determinants of population's $PM_{2.5}$ exposure risk in China, 1998–2017: A case study of the Beijing-Tianjin-Hebei region. *Environ. Sci. Pollut. Res.* **2020**, *27*, 31767–31777. [CrossRef] [PubMed]

12. Wang, J.; Lu, X.; Yan, Y.; Zhou, L.; Ma, W. Spatiotemporal characteristics of $PM_{2.5}$ concentration in the Yangtze River Delta urban agglomeration, China on the application of big data and wavelet analysis. *Sci. Total. Environ.* **2020**, *724*, 138134. [CrossRef] [PubMed]
13. Huang, C.; Liu, K.; Zhou, L. Spatio-temporal trends and influencing factors of $PM_{2.5}$ concentrations in urban agglomerations in China between 2000 and 2016. *Environ. Sci. Pollut. Res.* **2021**, *28*, 10988–11000. [CrossRef] [PubMed]
14. Han, L.; Zhou, W.; Li, W. City as a major source area of fine particulate ($PM_{2.5}$) in China. *Environ. Pollut.* **2015**, *206*, 183–187. [CrossRef] [PubMed]
15. Hao, Y.; Liu, Y.-M. The influential factors of urban $PM_{2.5}$ concentrations in China: A spatial econometric analysis. *J. Clean. Prod.* **2016**, *112*, 1443–1453. [CrossRef]
16. Wang, Q.; Kwan, M.-P.; Zhou, K.; Fan, J.; Wang, Y.; Zhan, D. The impacts of urbanization on fine particulate matter ($PM_{2.5}$) concentrations: Empirical evidence from 135 countries worldwide. *Environ. Pollut.* **2019**, *247*, 989–998. [CrossRef]
17. Shi, K.; Wang, H.; Yang, Q.; Wang, L.; Sun, X.; Li, Y. Exploring the relationships between urban forms and fine particulate ($PM_{2.5}$) concentration in China: A multi-perspective study. *J. Clean. Prod.* **2019**, *231*, 990–1004. [CrossRef]
18. Wang, Z.-b.; Fang, C.-l. Spatial-temporal characteristics and determinants of $PM_{2.5}$ in the Bohai Rim Urban Agglomeration. *Chemosphere* **2016**, *148*, 148–162. [CrossRef]
19. Wu, Q.; Guo, R.; Luo, J.; Chen, C. Spatiotemporal evolution and the driving factors of $PM_{2.5}$ in Chinese urban agglomerations between 2000 and 2017. *Ecol. Indic.* **2021**, *125*, 107491. [CrossRef]
20. Xu, F.; Qiu, X.; Hu, X.; Shang, Y.; Pardo, M.; Fang, Y.; Wang, J.; Rudich, Y.; Zhu, T. Effects on IL-1β signaling activation induced by water and organic extracts of fine particulate matter ($PM_{2.5}$) in vitro. *Environ. Pollut.* **2018**, *237*, 592–600. [CrossRef] [PubMed]
21. Song, C.; He, J.; Wu, L.; Jin, T.; Chen, X.; Li, R.; Ren, P.; Zhang, L.; Mao, H. Health burden attributable to ambient $PM_{2.5}$ in China. *Environ. Pollut.* **2017**, *223*, 575–586. [CrossRef] [PubMed]
22. Kaiser, J. Mounting Evidence Indicts Fine-Particle Pollution. *Science* **2005**, *307*, 1858–1861. [CrossRef]
23. Xu, M.-X.; Ge, C.-X.; Qin, Y.-T.; Gu, T.-T.; Lou, D.-S.; Li, Q.; Hu, L.-F.; Feng, J.; Huang, P.; Tan, J. Prolonged $PM_{2.5}$ exposure elevates risk of oxidative stress-driven nonalcoholic fatty liver disease by triggering increase of dyslipidemia. *Free. Radic. Biol. Med.* **2019**, *130*, 542–556. [CrossRef]
24. Liu, J.; Han, Y.; Tang, X.; Zhu, J.; Zhu, T. Estimating adult mortality attributable to $PM_{2.5}$ exposure in China with assimilated $PM_{2.5}$ concentrations based on a ground monitoring network. *Sci. Total. Environ.* **2016**, *568*, 1253–1262. [CrossRef]
25. Liu, L.; Yan, Y.; Nazhalati, N.; Kuerban, A.; Li, J.; Huang, L. The effect of $PM_{2.5}$ exposure and risk perception on the mental stress of Nanjing citizens in China. *Chemosphere* **2020**, *254*, 126797. [CrossRef]
26. Wang, F.; Qiu, X.; Cao, J.; Peng, L.; Zhang, N.; Yan, Y.; Li, R. Policy-driven changes in the health risk of $PM_{2.5}$ and O_3 exposure in China during 2013–2018. *Sci. Total. Environ.* **2021**, *757*, 143775. [CrossRef]
27. Song, Y.; Huang, B.; He, Q.; Chen, B.; Wei, J.; Mahmood, R. Dynamic assessment of $PM_{2.5}$ exposure and health risk using remote sensing and geo-spatial big data. *Environ. Pollut.* **2019**, *253*, 288–296. [CrossRef]
28. Fu, X.; Li, L.; Lei, Y.; Wu, S.; Yan, D.; Luo, X.; Luo, H. The economic loss of health effect damages from $PM_{2.5}$ pollution in the Central Plains Urban Agglomeration. *Environ. Sci. Pollut. Res.* **2020**, *27*, 25434–25449. [CrossRef]
29. Wang, H.; Gao, Z.; Ren, J.; Liu, Y.; Chang, L.T.-C.; Cheung, K.; Feng, Y.; Li, Y. An urban-rural and sex differences in cancer incidence and mortality and the relationship with $PM_{2.5}$ exposure: An ecological study in the southeastern side of Hu line. *Chemosphere* **2019**, *216*, 766–773. [CrossRef]
30. Chen, D.; Zhang, Y.; Yao, Y.; Hong, Y.; Guan, Q.; Tu, W. Exploring the spatial differentiation of urbanization on two sides of the Hu Huanyong Line—Based on nighttime light data and cellular automata. *Appl. Geogr.* **2019**, *112*, 102081. [CrossRef]
31. Chen, M.; Gong, Y.; Li, Y.; Lu, D.; Zhang, H. Population distribution and urbanization on both sides of the Hu Huanyong Line: Answering the Premier's question. *J. Geogr. Sci.* **2016**, *26*, 1593–1610. [CrossRef]
32. Qi, W.; Liu, S.; Zhao, M.; Liu, Z. China's different spatial patterns of population growth based on the "Hu Line". *J. Geogr. Sci.* **2016**, *26*, 1611–1625. [CrossRef]
33. Weixia, H.U.; Jiaming, L.I.U.; Ming, L.I. Exploration of substitute industry for Shanxi's coal economy: On the path of key scenic spots propelling regional economic development. *China Popul. Resour. Environ.* **2016**, *26*, 168–176.
34. Fang, C. Important progress and future direction of studies on China's urban agglomerations. *J. Geogr. Sci.* **2015**, *25*, 1003–1024. [CrossRef]
35. Wei, J.; Li, Z.Q.; Cribb, M.; Huang, W.; Xue, W.H.; Sun, L.; Guo, J.P.; Peng, Y.R.; Li, J.; Lyapustin, A.; et al. Improved 1 km resolution $PM_{2.5}$ estimates across China using enhanced space-time extremely randomized trees. *Atmos. Chem. Phys.* **2020**, *20*, 3273–3289. [CrossRef]
36. Liu, H.; Cui, W.; Zhang, M. Exploring the causal relationship between urbanization and air pollution: Evidence from China. *Sustain. Cities Soc.* **2022**, *80*, 103783. [CrossRef]
37. Liu, H.; Fang, C.; Zhang, X.; Wang, Z.; Bao, C.; Li, F. The effect of natural and anthropogenic factors on haze pollution in Chinese cities: A spatial econometrics approach. *J. Clean. Prod.* **2017**, *165*, 323–333. [CrossRef]
38. Lyu, W.; Li, Y.; Guan, D.; Zhao, H.; Zhang, Q.; Liu, Z. Driving forces of Chinese primary air pollution emissions: An index decomposition analysis. *J. Clean. Prod.* **2016**, *133*, 136–144. [CrossRef]
39. He, Q.; Gao, K.; Zhang, L.; Song, Y.; Zhang, M. Satellite-derived 1-km estimates and long-term trends of $PM_{2.5}$ concentrations in China from 2000 to 2018. *Environ. Int.* **2021**, *156*, 106726. [CrossRef]

40. He, W.; Meng, H.; Han, J.; Zhou, G.; Zheng, H.; Zhang, S. Spatiotemporal $PM_{2.5}$ estimations in China from 2015 to 2020 using an improved gradient boosting decision tree. *Chemosphere* **2022**, *296*, 134003. [CrossRef]
41. Wang, X.; Li, T.; Ikhumhen, H.O.; Sá, R.M. Spatio-temporal variability and persistence of $PM_{2.5}$ concentrations in China using trend analysis methods and Hurst exponent. *Atmos. Pollut. Res.* **2022**, *13*, 101274. [CrossRef]
42. Xu, Y.; Ying, Q.; Hu, J.; Gao, Y.; Yang, Y.; Wang, D.; Zhang, H. Spatial and temporal variations in criteria air pollutants in three typical terrain regions in Shaanxi, China, during 2015. *Air Qual. Atmos. Health* **2018**, *11*, 95–109. [CrossRef]
43. Zhang, L.; Yang, L.; Bi, J.; Liu, Y.; Toriba, A.; Hayakawa, K.; Nagao, S.; Tang, N. Characteristics and unique sources of polycyclic aromatic hydrocarbons and nitro-polycyclic aromatic hydrocarbons in $PM_{2.5}$ at a highland background site in northwestern China. *Environ. Pollut.* **2021**, *274*, 116527. [CrossRef]
44. Zhao, Y.; Wang, L.; Huang, T.; Tao, S.; Liu, J.; Gao, H.; Luo, J.; Huang, Y.; Liu, X.; Chen, K.; et al. Unsupervised $PM_{2.5}$ anomalies in China induced by the COVID-19 epidemic. *Sci. Total. Environ.* **2021**, *795*, 148807. [CrossRef]
45. Chu, B.; Zhang, S.; Liu, J.; Ma, Q.; He, H. Significant concurrent decrease in $PM_{2.5}$ and NO_2 concentrations in China during COVID-19 epidemic. *J. Environ. Sci.* **2021**, *99*, 346–353. [CrossRef]
46. Yang, K.; Wu, C.; Luo, Y. The impact of COVID-19 on urban $PM_{2.5}$—Taking Hubei Province as an example. *Environ. Pollut.* **2022**, *294*, 118633. [CrossRef]
47. Bai, Y.-Q.; Wang, Y.; Kong, S.-F.; Zhao, T.-L.; Zhi, X.-F.; Zheng, H.; Sun, X.-Y.; Hu, W.-Y.; Zhou, Y.; Xiong, J. Modelling the effect of local and regional emissions on $PM_{2.5}$ concentrations in Wuhan, China during the COVID-19 lockdown. *Adv. Clim. Chang. Res.* **2021**, *12*, 871–880. [CrossRef]
48. Wen, L.; Yang, C.; Liao, X.; Zhang, Y.; Chai, X.; Gao, W.; Guo, S.; Bi, Y.; Tsang, S.-Y.; Chen, Z.-F.; et al. Investigation of $PM_{2.5}$ pollution during COVID-19 pandemic in Guangzhou, China. *J. Environ. Sci.* **2022**, *115*, 443–452. [CrossRef]
49. Li, L.; Qian, J.; Ou, C.-Q.; Zhou, Y.-X.; Guo, C.; Guo, Y. Spatial and temporal analysis of Air Pollution Index and its timescale-dependent relationship with meteorological factors in Guangzhou, China, 2001–2011. *Environ. Pollut.* **2014**, *190*, 75–81. [CrossRef]
50. Luo, Y.; Zhao, T.; Yang, Y.; Zong, L.; Kumar, K.R.; Wang, H.; Meng, K.; Zhang, L.; Lu, S.; Xin, Y. Seasonal changes in the recent decline of combined high $PM_{2.5}$ and O3 pollution and associated chemical and meteorological drivers in the Beijing–Tianjin–Hebei region, China. *Sci. Total. Environ.* **2022**, *838*, 156312. [CrossRef]
51. Brønnum-Hansen, H.; Bender, A.M.; Andersen, Z.J.; Sørensen, J.; Bønløkke, J.H.; Boshuizen, H.; Becker, T.; Diderichsen, F.; Loft, S. Assessment of impact of traffic-related air pollution on morbidity and mortality in Copenhagen Municipality and the health gain of reduced exposure. *Environ. Int.* **2018**, *121*, 973–980. [CrossRef]
52. Amato, F.; Zandveld, P.; Keuken, M.; Jonkers, S.; Querol, X.; Reche, C.; Denier van der Gon, H.A.C.; Schaap, M. Improving the modeling of road dust levels for Barcelona at urban scale and street level. *Atmos. Environ.* **2016**, *125*, 231–242. [CrossRef]
53. Lee, J.-H.; Wu, C.-F.; Hoek, G.; de Hoogh, K.; Beelen, R.; Brunekreef, B.; Chan, C.-C. LUR models for particulate matters in the Taipei metropolis with high densities of roads and strong activities of industry, commerce and construction. *Sci. Total. Environ.* **2015**, *514*, 178–184. [CrossRef]
54. Luo, Z.; Wan, G.; Wang, C.; Zhang, X. Urban pollution and road infrastructure: A case study of China. *China Econ. Rev.* **2018**, *49*, 171–183. [CrossRef]
55. Nam, K.-M. Is spatial distribution of China's population excessively unequal? A cross-country comparison. *Ann. Reg. Sci.* **2017**, *59*, 453–474. [CrossRef]
56. Zhao, S.Y.; Feng, T.; Tie, X.X.; Long, X.; Li, G.H.; Cao, J.J.; Zhou, W.J.; An, Z.S. Impact of Climate Change on Siberian High and Wintertime Air Pollution in China in Past Two Decades. *Earths Future* **2018**, *6*, 118–133. [CrossRef]
57. Cohen, A.J.; Brauer, M.; Burnett, R. Estimates and 25-year trends of the global burden of disease attributable to ambient air pollution: An analysis of data from the Global Burden of Diseases Study 2015 (vol 389, pg 1907, 2017). *Lancet* **2018**, *391*, 1576. [CrossRef]
58. Dong, J.; Wang, Y.; Wang, L.; Zhao, W.; Huang, C. Assessment of $PM_{2.5}$ exposure risk towards SDG indicator 11.6.2—A case study in Beijing. *Sustain. Cities Soc.* **2022**, *82*, 103864. [CrossRef]
59. He, Q.; Huang, B. Satellite-based high-resolution $PM_{2.5}$ estimation over the Beijing-Tianjin-Hebei region of China using an improved geographically and temporally weighted regression model. *Environ. Pollut.* **2018**, *236*, 1027–1037. [CrossRef]
60. Li, R.; Cui, L.; Meng, Y.; Zhao, Y.; Fu, H. Satellite-based prediction of daily SO2 exposure across China using a high-quality random forest-spatiotemporal Kriging (RF-STK) model for health risk assessment. *Atmos. Environ.* **2019**, *208*, 10–19. [CrossRef]
61. Wang, H.; Li, J.; Gao, Z.; Yim, S.H.L.; Shen, H.; Ho, H.C.; Li, Z.; Zeng, Z.; Liu, C.; Li, Y.; et al. High-Spatial-Resolution Population Exposure to $PM_{2.5}$ Pollution Based on Multi-Satellite Retrievals: A Case Study of Seasonal Variation in the Yangtze River Delta, China in 2013. *Remote Sens.* **2019**, *11*, 2724. [CrossRef]
62. Song, R.-f.; Wang, D.-s.; Li, X.-b.; Li, B.; Peng, Z.-r.; He, H.-d. Characterizing vertical distribution patterns of $PM_{2.5}$ in low troposphere of Shanghai city, China: Implications from the perspective of unmanned aerial vehicle observations. *Atmos. Environ.* **2021**, *265*, 118724. [CrossRef]
63. Li, C.; Liu, M.; Hu, Y.; Zhou, R.; Huang, N.; Wu, W.; Liu, C. Spatial distribution characteristics of gaseous pollutants and particulate matter inside a city in the heating season of Northeast China. *Sustain. Cities Soc.* **2020**, *61*, 102302. [CrossRef]
64. Jerrett, M.; Turner Michelle, C.; Beckerman Bernardo, S.; Pope, C.A.; van Donkelaar, A.; Martin Randall, V.; Serre, M.; Crouse, D.; Gapstur Susan, M.; Krewski, D.; et al. Comparing the Health Effects of Ambient Particulate Matter Estimated Using Ground-Based versus Remote Sensing Exposure Estimates. *Environ. Health Perspect.* **2017**, *125*, 552–559. [CrossRef]

65. Miao, C.; Yu, S.; Hu, Y.; Bu, R.; Qi, L.; He, X.; Chen, W. How the morphology of urban street canyons affects suspended particulate matter concentration at the pedestrian level: An in-situ investigation. *Sustain. Cities Soc.* **2020**, *55*, 102042. [CrossRef]
66. He, Q.; Zhang, M.; Song, Y.; Huang, B. Spatiotemporal assessment of $PM_{2.5}$ concentrations and exposure in China from 2013 to 2017 using satellite-derived data. *J. Clean. Prod.* **2021**, *286*, 124965. [CrossRef]
67. Setton, E.; Marshall, J.D.; Brauer, M.; Lundquist, K.R.; Hystad, P.; Keller, P.; Cloutier-Fisher, D. The impact of daily mobility on exposure to traffic-related air pollution and health effect estimates. *J. Expo. Sci. Environ. Epidemiol.* **2011**, *21*, 42–48. [CrossRef]
68. Dewulf, B.; Neutens, T.; Lefebvre, W.; Seynaeve, G.; Vanpoucke, C.; Beckx, C.; Van de Weghe, N. Dynamic assessment of exposure to air pollution using mobile phone data. *Int. J. Health Geogr.* **2016**, *15*, 14. [CrossRef]
69. Rout, A.; Nitoslawski, S.; Ladle, A.; Galpern, P. Using smartphone-GPS data to understand pedestrian-scale behavior in urban settings: A review of themes and approaches. *Comput. Environ. Urban Syst.* **2021**, *90*, 101705. [CrossRef]
70. Wang, H.; Tang, R.; Liu, Y. Potential Health Benefit of NO2 Abatement in China's Urban Areas: Inspirations for Source-specific Pollution Control Strategy. *Lancet Reg. Health—West. Pac.* **2022**, *24*, 100482. [CrossRef]
71. Zhu, S.; Xia, L.; Wu, J.; Chen, S.; Chen, F.; Zeng, F.; Chen, X.; Chen, C.; Xia, Y.; Zhao, X.; et al. Ambient air pollutants are associated with newly diagnosed tuberculosis: A time-series study in Chengdu, China. *Sci. Total. Environ.* **2018**, *631–632*, 47–55. [CrossRef]